


## Article

# Effect of Rigid Aquatic Bank Weeds on Flow Velocities and Bed Morphology

Elzahry Farouk M. Elzahry<sup>1</sup>, Mahmoud Ali R. Eltokhy<sup>1</sup>, Mohamed S. Abdelmoaty<sup>2</sup>, Ola Mohamed Eraky<sup>2</sup> and Ibrahim G. Shaaban<sup>3,\*</sup> 

<sup>1</sup> Civil Engineering Department, Shoubra Faculty of Engineering, Benha University, Shoubra 11629, Egypt; alzahry.alzahry@feng.bu.edu.eg (E.F.M.E.); mahmoud.altokhy@feng.bu.edu.eg (M.A.R.E.)

<sup>2</sup> Channel Maintenance Research Institute, National Water Research Center (NWRC), Cairo 13621, Egypt; m\_abdelmoaty@nwrc.gov.eg (M.S.A.); ola\_eraky@nwrc.gov.eg (O.M.E.)

<sup>3</sup> Civil Engineering Department, School of Computing and Engineering, University of West London, London W5 5RF, UK

\* Correspondence: ibrahim.shaaban@uwl.ac.uk

**Abstract:** The prediction of changes in velocity distribution and channel bed morphology is significant in open channel management and design. This paper implements experimental work to realize and quantify the effect of rigid aquatic bank weeds on vertical velocity profiles and channel bed morphology. In the experimental work, weeds were given a staggered distribution using three distances of 25, 50, and 75 mm, unilaterally and bilaterally, with Froude numbers ranging from 0.11 to 0.30, achieving 168 scenarios. Results for the tested weed cases showed that the average velocity was directly proportional to the weed density and approached the Froude number. By comparing the smooth and weeded velocities, it was found that the velocity inside the infested reach was close to the downstream velocity and exceeded the upstream velocity by about 10% and 41%, respectively. Scour depths along the centerline of the vegetated reach for the bilateral weeds were higher by 11% to 33% than those for the unilateral weeds. The maximum observed depth of the scour holes along the smooth bank was about 30% to 60% of the maximum scour depth at the middle line. Finally, to quantify the results, multiple regression analysis was performed to develop empirical equations to assist in the water management process.

**Keywords:** side vegetation; density; velocity profile; scour depth



**Citation:** Elzahry, E.F.M.; Eltokhy, M.A.R.; Abdelmoaty, M.S.; Eraky, O.M.; Shaaban, I.G. Effect of Rigid Aquatic Bank Weeds on Flow Velocities and Bed Morphology. *Water* **2023**, *15*, 3173. <https://doi.org/10.3390/w15183173>

Academic Editor: Achim A. Beylich

Received: 22 July 2023

Revised: 23 August 2023

Accepted: 31 August 2023

Published: 5 September 2023



**Copyright:** © 2023 by the authors. Licensee MDPI, Basel, Switzerland. This article is an open access article distributed under the terms and conditions of the Creative Commons Attribution (CC BY) license (<https://creativecommons.org/licenses/by/4.0/>).

## 1. Introduction

Aquatic weeds exist in waterways in different forms, which can be classified according to their position as submerged, emergent, and bank weeds [1]. Weeds can also be classified, according to their flexibility, as rigid or flexible [1]. Current research is focused on rigid bank weeds. The excessive existence of these weeds in irrigation channels causes many hydraulic problems by changing the flow properties of the infested channels [2]. Recently, researchers found that the effect of ditch-bank weeds is dissimilar to the effect of weeds on the channel bed, as ditch-bank weeds promote geomorphic stability through increasing flow resistance, thus reducing near-bank flow velocity [3–5]. Therefore, the concept of ditch-bank weeds and their effects on main channel flow properties must be developed, and several more studies should be carried out to understand and clarify the effect of ditch-bank weeds on flow characteristics.

In open channels, the velocity distribution and the change in bed morphology are two issues for the same concept, in which velocity is an indicator of morphological change. The presence of aquatic weeds in the irrigation channel changes the channel flow velocities and can thus affect the bed scour and the channel morphology. In addition, aquatic weeds can change the particle movement pattern of the bed soil [6,7].

Hopkinson and Wynn [8] studied the effect of bank weeds’ stiffness on velocity distribution experimentally. The results concluded that, for all cases, the velocity near the bank weeds was lower than the velocity in the middle of the channel. Afzalimehr and Dey [9], Hirschowitz and James [10], Afzalimehr et al. [11], Mohammadzade et al. [12], Liu et al. [13], Valyrakis et al. [14], and Eraky et al. [15] experimentally studied the effect of rigid bank-weed density on flow velocities, showing that bank weeds obstruct the flow, causing an increase in velocity in mid-channel and reducing it near the bank.

James et al. [16], Hirschowitz and James [10], Huai et al. [17], Valyrakis et al. [14], and Liu and Shan [18] used experimental and numerical models to predict empirical equations to determine the vegetation velocity ( $V_v$ ) for emerged weeds (Table 1).

**Table 1.** Prediction equations for mean velocity due to emerged vegetation velocity.

Authors	Equation	Remark
James et al., 2004 [16]	$V_v = \frac{1}{F} \sqrt{S}$ $F = \sqrt{\frac{2g}{C_d N d}} \sqrt{\left(1 - \frac{N\pi d^2}{4}\right)}$	F: resistance coefficient accounting for stem drag; S: channel slope; N: number of stems per unit area; d: stem diameter; C <sub>d</sub> : drag coefficient.
Hirschowitz and James 2009 [10]	$V_v = \left(\frac{gA}{\frac{f_b}{8} B + 2 \frac{f_v}{8} h}\right)^{0.5} S^{0.5}$	A: cross-sectional area of the un-vegetated zone; B: bed width; h: flow depth at the interface; f <sub>b</sub> : friction factor of the bed; f <sub>v</sub> : friction factor of the vegetation interface.
Huai et al., 2009 [17]	$V_v = \sqrt{\frac{2gi}{C_d m D}}$	D: cylinder diameter. m: number of stems in the control volume = 1/(x <sub>a</sub> y <sub>a</sub> ); i: energy slope.
Valyrakis et al., 2021 [14]	$V_v = u (1 - 0.143 \varphi)$	φ: solid volume fraction ( $\varphi = m\pi D^2 / (4LW_v)$ ); u: mean velocity in the no-weeds case.
Liu and Shan 2022 [18]	$V_v = \sqrt{\left(\frac{ghS}{C_f + 0.5 (C_d ah (1-\varphi))}\right)}$	S: water surface slope; Φ: solid volume fraction ( $=(\pi/4)nd^2$ ); C <sub>f</sub> : bed friction coefficient; C <sub>d</sub> : drag coefficient; a: frontal area per patch volume ( $=nd$ ); h: flow depth.

Lately, several experimental studies have been established to investigate the effects of flexible and rigid bank vegetation on channel morphology. Van de Lageweg et al. [19] and Yang et al. [20] studied the impact of flexible bank vegetation on channel patterns and meandering dynamics using three vegetation densities. The results concluded that higher vegetation density led to increased bank strength. However, for low vegetation density, the erosion was locally enhanced. According to Abdelhaleem et al., a scour depth empirical equation can be estimated from experimental data by using non-linear regression analysis [21].

Li et al. [22] experimentally studied the effect of bank weeds on erosion and deposition. The study concluded that the maximum erosion always occurred within the first 3 h of the experiments. After that, the development and recovery stage began between 3 and 6 h, followed by a deposition stage 6 h after the beginning. Also, the results showed that, for weed densities of more than 100 stems/m<sup>2</sup>, there was no significant difference between the scouring stage and the development stage.

Vargas-Luna et al. [23] studied the impact of rigid bank vegetation on channel patterns using only one density and a D<sub>50</sub> equal to 0.50 mm. The results concluded that bank vegetation reduced scour near banks. Also, Vargas-Luna et al. [24] experimentally concluded that, at variable discharge, vegetation establishment on floodplains reduced bank erosion. Azarisamani et al. [25] studied the physical effects of rigid vegetation distribution on bed

scouring at the toe and bank slope of a meandering river. The results concluded that, in the presence of vegetation, the core of maximum velocity diverted toward the centerline of the flume, reducing erosion risk.

In experimental work, vegetation is generally distributed as linear or staggered, but from the authors' point of view, staggered distribution is closer to natural distribution, although in a regular shape that can be simulated and tested. In addition, the staggered configuration allows more resistance to the flow by diffusing energy and reducing velocity near the vegetation, as presented in [26–28]. They experimentally found that the staggered configuration enhanced the flow resistance more than the linear array did.

The simulation of rigid vegetation has been represented in several previous studies describing the properties and configuration of the simulated vegetation (e.g., material used, thickness, and spacing). A summary review of rigid-weed simulations from the studies [29–40] was conducted, as shown in Table 2, to help select a suitable weed simulation for this research.

**Table 2.** Summary of rigid vegetation simulations.

Authors	Stem Simulation				
	Shaped	Material	Diameter (mm)	Spacing ( $\Delta x$ )	Distribution
James et al. [16]	Cylindrical	Steel	5	2.5, 5, and 7.5 cm	Staggered
Stone and Shen [28]		Wood	3.18, 6.35 and 12.7	3.8, 4.6 and 7.6 cm	Staggered
Meftah et al. [29]		Steel	3	10 cm	Linear
Kothyari et al. [30]		Stainless steel	10	3.2 to 20.3 cm	Staggered
Cheng and Nguyen [31]		Steel	3.2, 6.6 and 8.3	3 and 6 cm	Staggered
Panigrahi [32]		Steel	6.5	10 cm	Both linear and staggered
Ahmed and Hady [33]		PVC	10	22.72, 11.9, and 9.61 cm	Linear
Chakraborty and Sarkar [34]		PVC	6	Random Distribution	
Tong et al. [35]		PVC	8	10 cm	Linear
D'Ippolito et al. [36]		Wood	8 and 10	4.24 and 8.48 cm	Both linear and staggered
Lee et al. [37]		Acrylic	10	4 and 8 cm	staggered
Wang et al. [38]		PVC	6	6 cm	Linear
Huang et al. [39]		Wood	6	2.5 and 5 cm	Linear
Current study		Steel	3	2.5, 5, and 7.5 cm	Staggered

Recently, Li et al. [41] numerically studied the effect of one-sided bank vegetation on morphological change. The results showed that the vegetation pushed the flow toward the opposite bank and caused localized bank erosion. Lin et al. [42] numerically and experimentally deduced the effect of emerged bank weeds on the velocity profiles. They concluded that the emerged bank weeds reduced the velocity near the bank and that the level of velocity reduction was proportional to the weed density due to the high drag of the weeds. Mofrad et al. [42] presented an experimental comparison between the vegetation on the channel bed and the channel banks and their effects on the velocity distribution. The study proved that, in the case of the submerged vegetation (i.e., the bed vegetation), the location of maximum velocity was observed near the water surface. However, for the emergent vegetation (i.e., the bank vegetation), the maximum velocity was shifted towards the bed due to the generation of secondary flow. The study recommended a better estimation of the effects of bank weeds on the hydraulic parameters and morphological change; this plays a role in reducing the cost of channel maintenance projects and modifying the input data for hydraulic models.

Most of the previous studies were focused on visualizing the effect of aquatic bank weeds on velocity and bed morphology, without paying significant attention to quantifying these visualizations for different vegetation densities and Froude numbers.

Therefore, the motivation of the current study is to experimentally explore the effect of rigid bank-weed density on velocity distributions and changes in bed morphology under different flow conditions. The experiments were conducted using different Froude numbers under subcritical flow conditions for clear water.

## 2. Methods and Materials

### 2.1. Dimensional Analysis

Dimensional analysis was used to derive a general equation that related the independent variables to the dependent variables. A general relationship between the change in water velocity and scour depth (dependent variables) and both the vegetation density and the approached Froude number (independent variables) was deduced as follows:

$$f(\lambda, V_u, V_d, V_{in}, u, \bar{u}, (ds)_{max}, g, \rho, \mu, y_o) = 0 \quad (1)$$

where  $\lambda$  is the weed density  $= \pi N_o d^2/4$ , ( $N_o$  is the number of stems per unit side area, and  $d$  is the stem diameter (m)),  $V_u$  is the upstream velocity (m/s),  $V_d$  is the downstream velocity (m/s),  $V_{in}$  is the velocity in the middle of the infested reach (m/s),  $u$  is the smooth velocity (m/s),  $\bar{u}$  is the average velocity in the smooth case (m/s),  $(ds)_{max}$  is the maximum scour depth inside the weedy reach (m),  $g$  is the gravitational acceleration ( $m/s^2$ ),  $\rho$  is the density of water,  $\mu$  is the dynamic viscosity of water, and  $y_o$  is the smooth water depth (m). By using Buckingham's Pi theorem, the general equation can be modified as follows:

$$f(V_u/u, V_d/u, V_{in}/u, (ds)_{max}/y_o) = (\lambda, F_{ro}) \quad (2)$$

where  $F_{ro}$  is the approached Froude number,  $F_{ro} = \bar{u}/(g y_o)^{1/2}$ .  $R_n$  is the Reynolds number, where  $R_n = [(\rho g^{1/2} y_o^{3/2})/\mu]$  for free-surface open-channel flow;  $R_n$  is in the fully turbulent zone and has a negligible effect.

### 2.2. Experimental Setup

The experimental runs were carried out using the reinforced concrete trapezoidal cross-section flume of a recirculating water supply system. The main part of the flume had dimensions of 16.22 m length, 0.60 m bed width, a maximum depth of 0.42 m, and a 1:1 side slope. The water depth in the flume was controlled using a revolving gate at the end of the flume. An underground reservoir with dimensions of 24.10 m long, 1.75 m wide, and 1.50 m deep was used for water supply and sand deposition to ensure clear water range. Also, two 5-inch centrifugal pumps were used to re-pump the flow from the underground reservoir.

The summary review of rigid weed simulation (Table 2) shows that weed stems were represented in this study as steel rods with a diameter of 3 mm, arranged in a staggered grid pattern and fixed in the middle 4 m of the flume length. Weeds were distributed to simulate unilateral and bilateral infestation, as shown in Figure 1, with three center spacings of 25, 50, and 75 mm in both the longitudinal and transverse directions. The rods were secured above a steel panel with drilled holes. Three densities of ditch-bank weeds of 1600, 400, and 178 stem/m<sup>2</sup> and three weed densities,  $\lambda$ , of 0.013, 0.0028, and 0.0013/m were used.

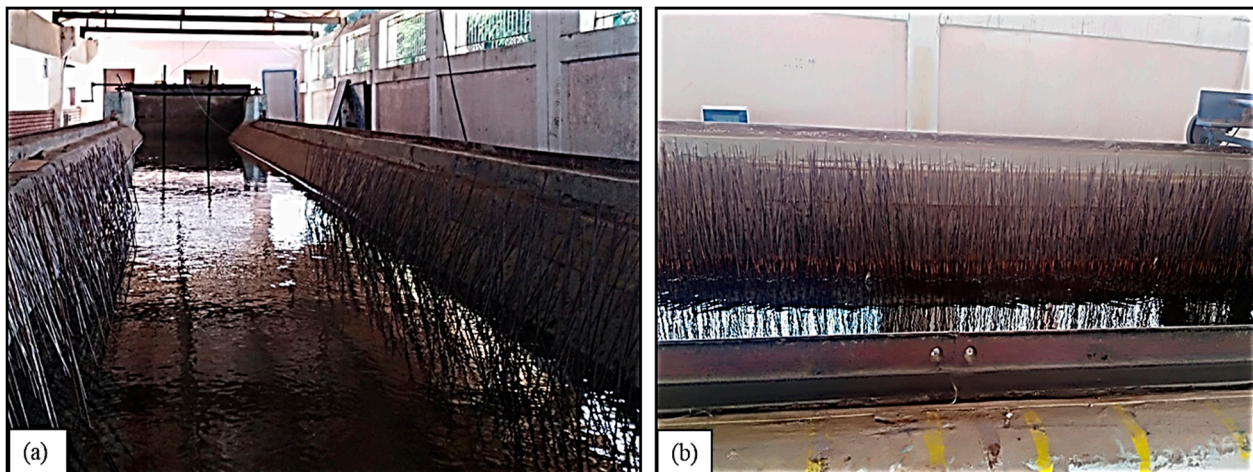


**Figure 1.** Artificial flume, rigid vegetation on the channel side slopes: (a) bilateral weeds; (b) unilateral weeds.

To study the effect of bank weeds on bed morphology, a sand soil basin was constructed within the infested reach with the same flume width of 60 cm and length of 4.00 m, equal to that of the infested reach. The sand basin had a depth of 30 cm and was filled with sand with a median grain size of  $D_{50} = 0.65$  mm. The geometrical standard deviation of the used sand,  $\sigma_g = (D_{84}/D_{16})^{1/2} = 1.37 < 1.40$ , indicated that the used bed material was uniform; Dey et al. [43]. The grain size distribution for the used sand was presented in Figure 2. A drainage system was installed on the bottom of the sand basin to drain excess water before surveying sand surface levels at the end of each run. Before each run, the basin was refilled with the sand and leveled to the bed level—i.e., all runs had the same experimental work conditions and started with the same sediment bed height.

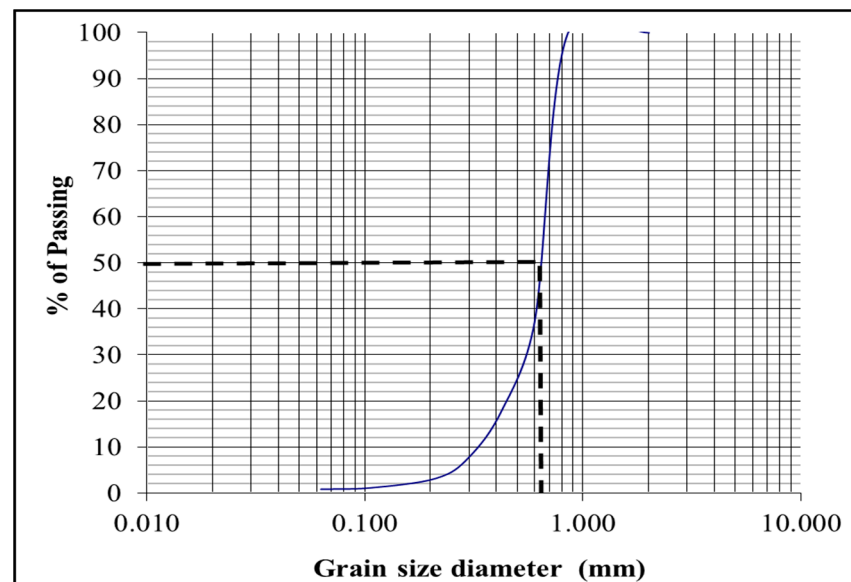


**Figure 2.** Grain size distribution of the used sand bed.

The flowing discharge was measured using two-channel electronic flow meters of the “Controlotron system 1010 P universal portable flow meter” type. The vertical velocity profile was measured using a Vectrino 3-D water velocity sensor. Additionally, the formed bed scour holes were surveyed using a point gauge with a 0.01 cm accuracy to determine the scour depth.

Different simulation scenarios were run to investigate the effect of rigid ditch-bank weeds on water surface profile, velocity, bed morphology, and subcritical flow in trapezoid open channels at different discharges and weed densities. The effect of weed densities was tested using four different discharges of 25, 30, 35, and 40 L/s and three different tail water depths at Froude numbers ranging from 0.11 to 0.30, achieving 168 scenarios, as shown in Table 3.

Table 3. Experimental conditions/limitations.

Weeds Configuration			Bed Condition	Discharge (L/s)	Tail Water Depth	No of Runs
Density/m	Arrangement	Spacing cm				
No weeds	n/a	n/a	concrete	40,35,30,25 L/s	Three different tail depths for each discharge	12
High ( $\lambda \sim 0.013$ )	Staggered both bilateral and unilateral weeds	2.5		40,35,30,25 L/s		24
Medium ( $\lambda \sim 0.0028$ )		5.0		40,35,30,25 L/s		24
Low ( $\lambda \sim 0.0013$ )		7.5		40,35,30,25 L/s		24
No weeds	n/a	n/a	Sandy soil with $D_{50} = 0.65$	40,35,30,25 L/s		12
High ( $\lambda \sim 0.013$ )	Staggered both bilateral and unilateral weeds	2.5		40,35,30,25 L/s		24
Medium ( $\lambda \sim 0.0028$ )		5.0		40,35,30,25 L/s		24
Low ( $\lambda \sim 0.0013$ )		7.5		40,35,30,25 L/s		24
Total Number of Runs						168

As Table 3 shows, the experiments were divided into two sets. The first set, in a fixed bed (concrete), was used during velocity measurements to achieve similar conditions when comparing the upstream, inside, and downstream velocity profiles and to avoid the effect of turbulent soil movement.

Before measuring the velocity, the vegetation density was adjusted according to the run specification. The flow stability should be ensured by leaving an indefinite amount of time before the measuring process in order to achieve the experimental boundary condition mentioned in Table 3 and a measuring discharge equal to that required; the depth of water just upstream of the tailgate was the required depth.

After that, the water level along the flume was measured by using an ultrasonic level meter, and the height-flow stability was checked at the same time. Then, the velocity profiles were measured upstream, downstream, and in the middle of the weedy reach along the flume centerline, as shown in Figure 3.

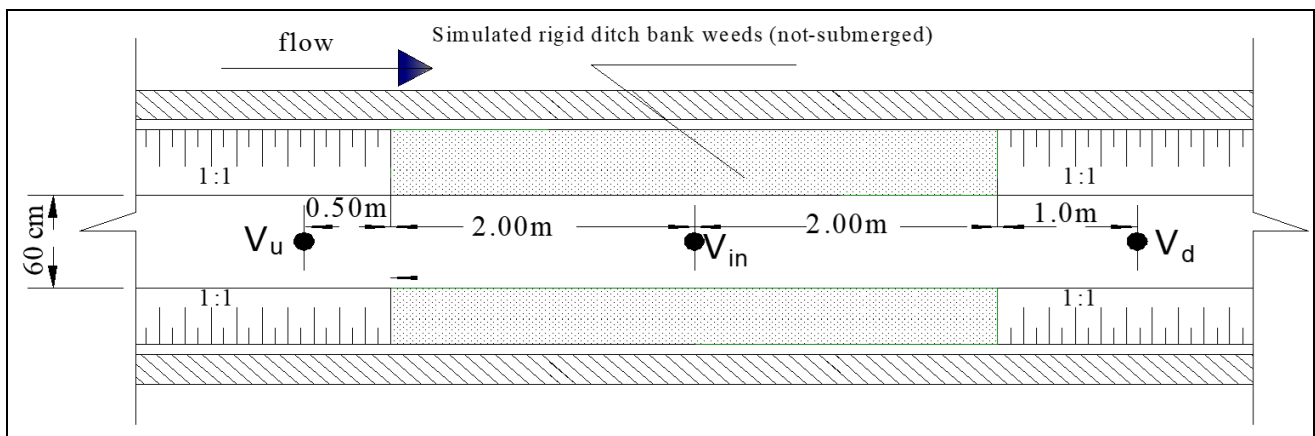


Figure 3. Locations for measuring vertical velocity profiles.

In the second set of experiments, a movable bed (sand) along the infested reach was used during scour measurements. In this stage, each experimental run consisted of the following steps:

- The sand basin was filled with the tested sand and leveled to the channel bed level.
- The vegetation density and tail-water depth were adjusted according to the study run.
- The flume was filled to the required level by making the pumps circulate the flow very slowly until the flow was adjusted to the required value (25, 30, 35, and 40 L/s) using the control valve.
- The experiment was run for the equilibrium time, which was estimated later, and then the feeding pump was turned off.
- Water was drained out slowly until the formed sand holes became visible.
- Bed scour holes were surveyed every 0.16 and 0.12 m in the longitudinal and transverse directions, respectively.

### 3. Results and Discussion

First, trial experimental runs were conducted under a clear water range to determine the required time at which the quasi-equilibrium state was reached. Generally, as shown in Figure 4, the scour depths increased with time all over the infested reach, but in some locations the scour depths fluctuated (increased or decreased) around the equilibrium. This is attributed to the effect of vegetation on the flow field.

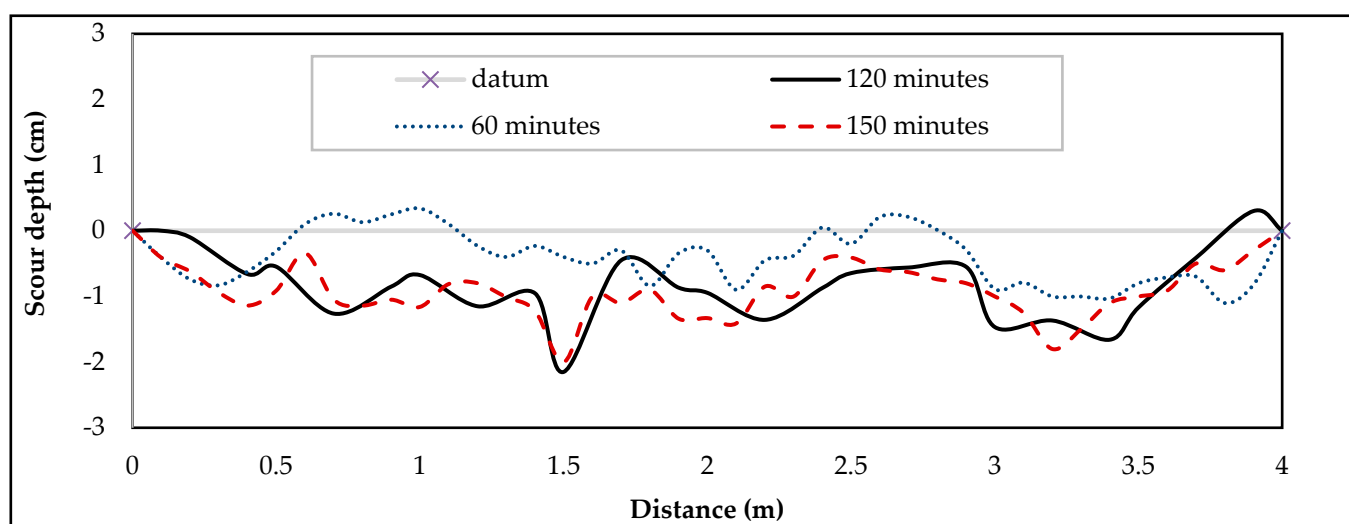


**Figure 4.** Scour depth along the centerline of the weedy reach.

The results showed that the equilibrium time for each run was almost reached at three hours because the shape of the scour hole and maximum depths of scour are almost the same at 2 and 2.5 h—those values are consistent with Li et al. [22]. The effects of rigid aquatic bank weeds on flow–velocity distribution and bed morphology are discussed below.

#### 3.1. Vertical Velocity Profile

One of the main motivations for the current research was to investigate the effects of bank vegetation on velocity upstream, inside, and downstream of the vegetation reach. Consequently, the velocity locations were selected at the most critical points. The water surface profile was measured for each case. The locations of  $V_u$ ,  $V_{in}$ , and  $V_d$  were decided according to the essential location at which the behavior of the water surface changed due to vegetation (see Figure 3). The vertical velocity profile was measured every 2 cm to predict the vertical profiles. In some cases, three distributed cross-sections of the velocity profile were measured at the center of the infested reach, with one in the middle, one near

the right bank, and the other near the left bank. These measurements aimed to visualize the effect of the bank vegetation on velocities near the bank.

The measured vertical velocity profiles were for the different weed densities and arrangements shown in Figures 5 and 6. It was observed that the maximum velocity in the center of the infested reach occurred at the lower half of the water column ( $y/h_o \leq 0.5$ ), where bank weed presence produced secondary flow that increased the velocity near the channel bed. As a result of that, the approach of logarithmic distribution was achieved only until  $y/h_o \leq 0.5$  for  $W/h \leq 3$ , “where  $W/h$  is the ratio between the channel width and the flow height”. These results agreed with the findings of [9,11–13,15,30,44], which concluded that, in the presence of vegetation on the channel walls, the level of maximum velocity and maximum shear stress is below the water surface and occurs near the channel bed. Also, Afzalimehr and Dey [9] observed that the maximum velocity is located at  $y/h_o = 0.2$ , near the vegetated bank, and at  $y/h_o = 0.56$  in the flume center under uniform flow and an aspect ratio of ( $W/h = 3$ ). Also, it was found that for all weed densities, the maximum velocity  $V_{max}$  was higher than that in the smooth case (no weeds). The maximum velocity-increasing ratios ( $V_{max}/u_{max}$ ) were recorded in Table 4.

It was noticed that the velocity in bilateral infestation cases was higher than that in unilateral infestation cases, i.e., the distribution of weeds on both sides had the most significant effect on flow velocity. By comparing the smooth velocity to the velocity in the presence of weeds, it was found that the velocity inside the infested reach was close to the downstream velocity and more than the upstream velocity by about 10% and 41%, respectively. Devi and Kumar [44] found that the downstream velocity was more than the velocity upstream of the weeds by about 16%. Furthermore, for all study cases, the average velocity was directly proportional to both the weed density ( $\lambda$ ) and Froude number ( $F_{ro}$ ).

The reliability of the measured velocity inside the infested reach ( $V_{in}$ ) was examined using 36 data points to re-determine it using the predictor equations of James et al. [16], Hirschowitz and James [10], Huai et al. [17], Valyrakis et al. [14], and Liu and Shan [18]. Figure 7 plots the measured velocities inside the weedy reach and those calculated by the above-mentioned equations in Table 1.

An error statistical analysis was conducted to evaluate the models used and check the validity of the measured velocities. Table 4 shows the error statistics for different equations using current experimental datasets. It was observed that the study conducted by [14] and the current research shared similar procedures and objectives, and, as a result, the predicted velocity from [14] showed the same trend as the measured velocity in addition to a small RMSE. Therefore, this was the most adequate approach to the research results.

Hirschowitz [10,16,18] experimentally studied the hydraulic effect of emerged rigid vegetation distributed along the channel bed. Although the presented research was interested in the emerged bank vegetation, the estimated equations from [10,16,18] had a small RMSE. Although a higher RMSE had been observed when testing the reliability of the equation of Huai et al. 2009 [17], this may be because the model equation was based on a numerical model and also concerns the vegetation on the channel bed.

**Table 4.** The maximum velocity-increasing ratios ( $V_{max}/u_{max}$ ).

Arrangement	Density	Velocity Position		
		Upstream	Middle	Downstream
Bilateral infestation	High	9%	50%	43%
	Medium	4%	32%	28%
	Low	2%	27%	24%
Unilateral infestation	High	4%	24%	17%
	Medium	2%	12%	9%
	Low	1.4%	12%	8%



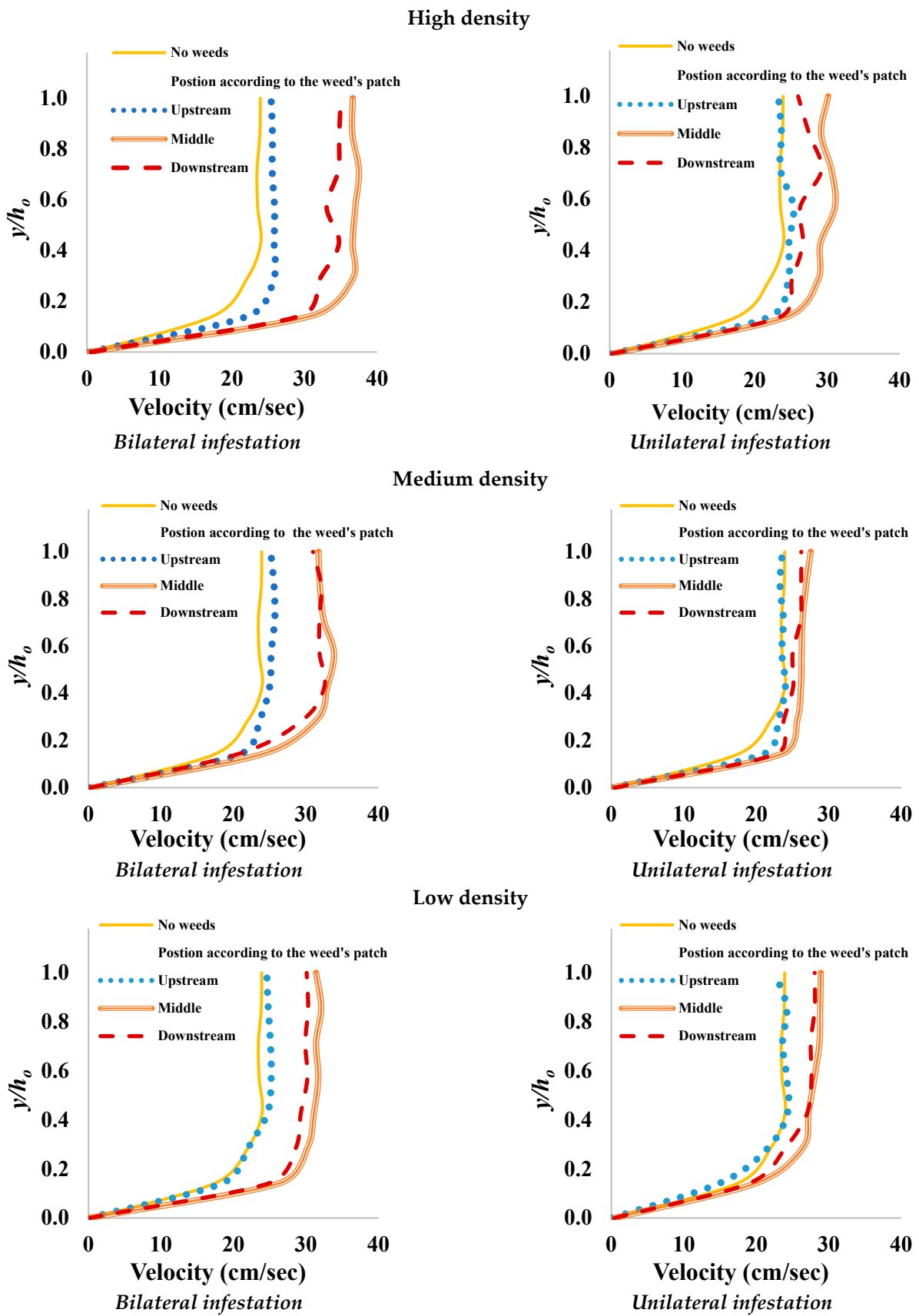


Figure 5. Vertical velocity profiles for both bilateral and unilateral arrangements at  $F_{r0} = 0.15$ .

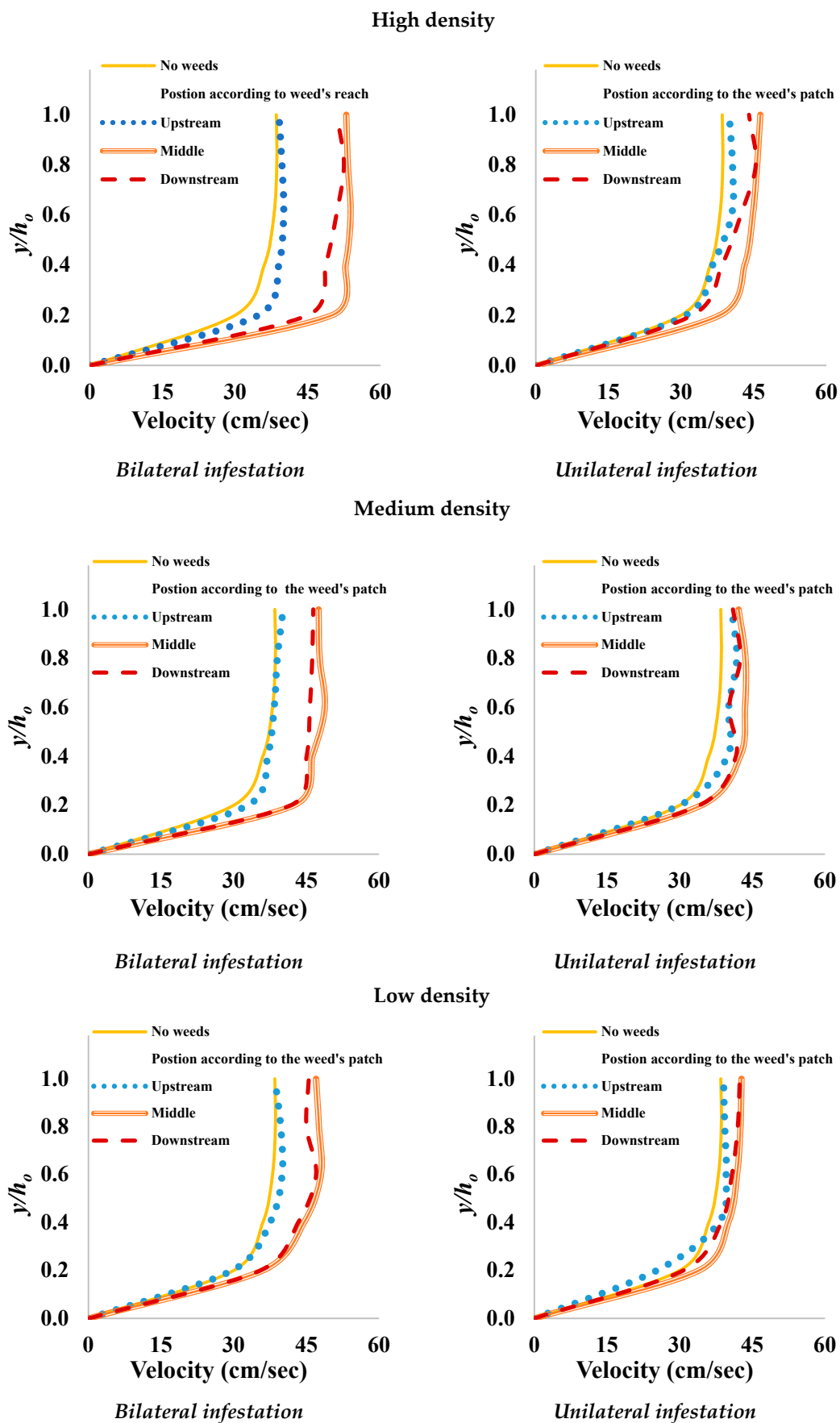
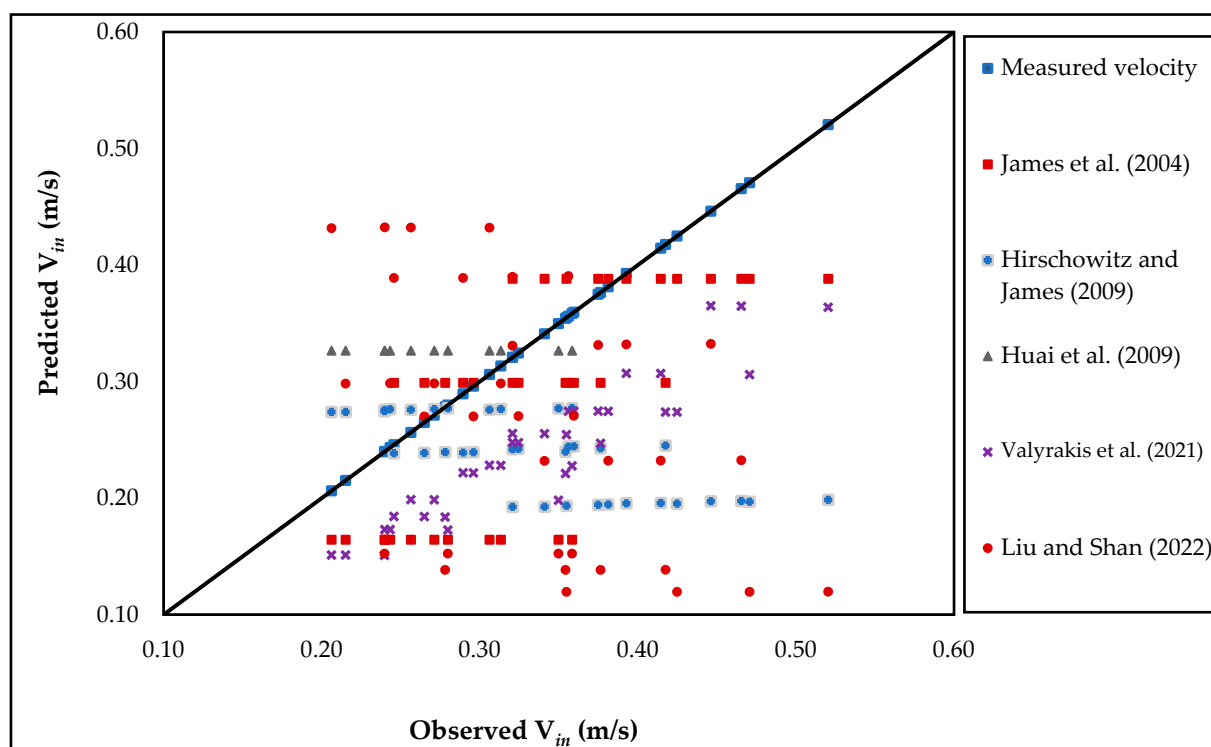


Figure 6. Vertical velocity profiles for both bilateral and unilateral arrangements at  $F_{r0} = 0.30$ .



**Figure 7.** Measured velocities inside the infested reach versus those predicted using the literature equations in Table 1 [10,14,16–18].

Table 5 shows that all the models under-predicted the velocity inside the weedy reach and performed well with the measured data in this experimental work. The model of Huai, W. X et al. [17] has the maximum error estimation, possibly because the model equation was based on a numerical model.

**Table 5.** Error statistics for the literature equations using measured experimental datasets.

Authors/Model	Average Error	Maximum Error	Minimum Error	Variance	RMSE
James et al. [16]	−0.189	0.080	−0.043	0.018	0.080
Hirschowitz and James [10]	−0.322	0.068	−0.098	0.018	0.141
Huai et al. [17]	−0.014	0.493	0.259	0.053	0.299
Valyrakis et al. [14]	−0.165	−0.055	−0.095	0.019	0.100
Liu and Shan [18]	−0.400	0.247	−0.062	0.022	0.175

To study the velocity variation between the middle and near the bank, velocities were measured at the vertical profile positions shown in Figure 8. From the vertical velocity profiles plotted in Figure 9, it was observed that the weeds on the channel sides obstructed and pushed the flow to the middle, causing the velocity in the middle to be greater than that near the bank. For a unilateral infestation, the velocity near the smooth side was higher than the velocity near the weedy side. Therefore, it can be concluded that, in cases of bilateral weeds, the flow is concentrated in the middle part of the infested reach, while in the case of unilateral weeds, the pushing flow is distributed between the middle and the smooth side.

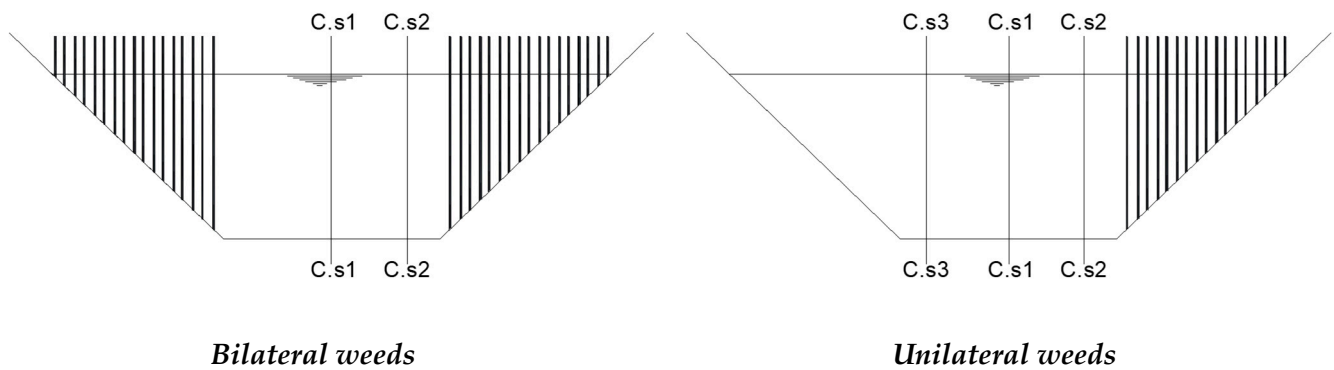


Figure 8. Definition sketch for different middle velocity cross-sections.

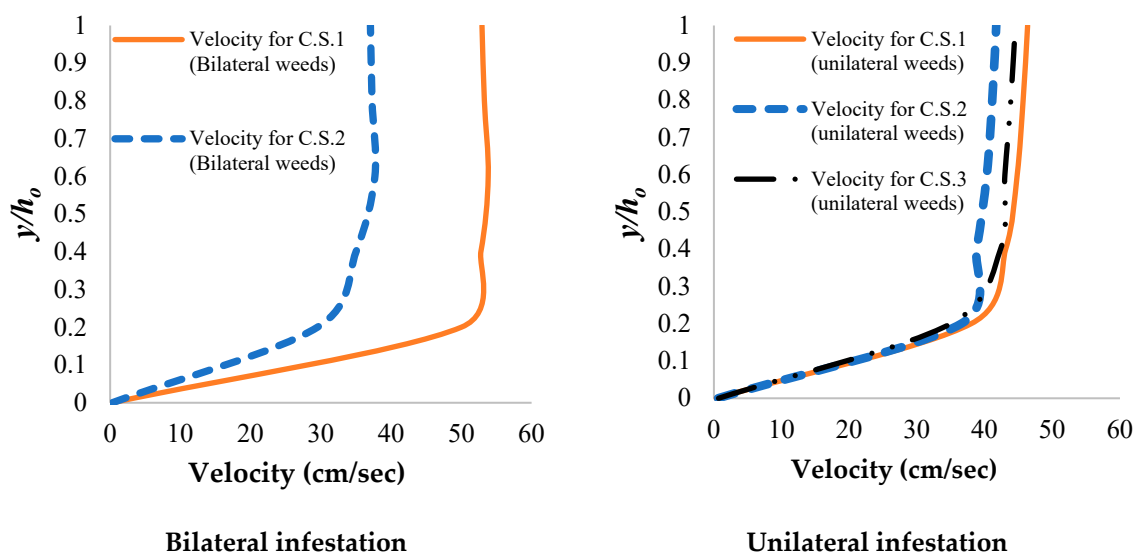


Figure 9. Definition sketch for different middle-velocity cross-sections.

### 3.2. Bed Morphology

The second purpose of this paper was to study the effect of rigid aquatic bank weeds on bed morphology. To illustrate this, some samples of the experimental run results were represented as contour maps and wireframe maps, as shown in Figures 10–13.

From the previous figures, it was noted that weeds on the canal’s side slope push the flow toward the canal center, causing the velocity in the center to be greater than that in the region near the bank, in turn leading to increased scouring along the middle of the weedy reach. In addition, some sediment areas were observed near the infested weed bank. So, it can be concluded that the presence of bank weeds helps protect the canal’s side slopes from erosion. This result was supported by several experimental works (Van de Lageweg et al. [19]; Amir et al. [45]; Yang et al. [20]; Vargas-Luna et al. [24]; Jumain et al. [27]). All these experiments agreed that the presence of weeds on a canal’s side slope/near the bank protected the side slopes/bank from erosion and maintained their stabilization.

For unilateral configuration, the flow was pushed from the infested side to the opposite smooth side, causing scour holes along the smooth side in addition to those in the middle section. Due to the pushing flow, the smooth bank was exposed to erosion, and the maximum observed scour hole depth along the smooth bank was about 30% to 60% of the maximum scour depth occurring at the middle line.

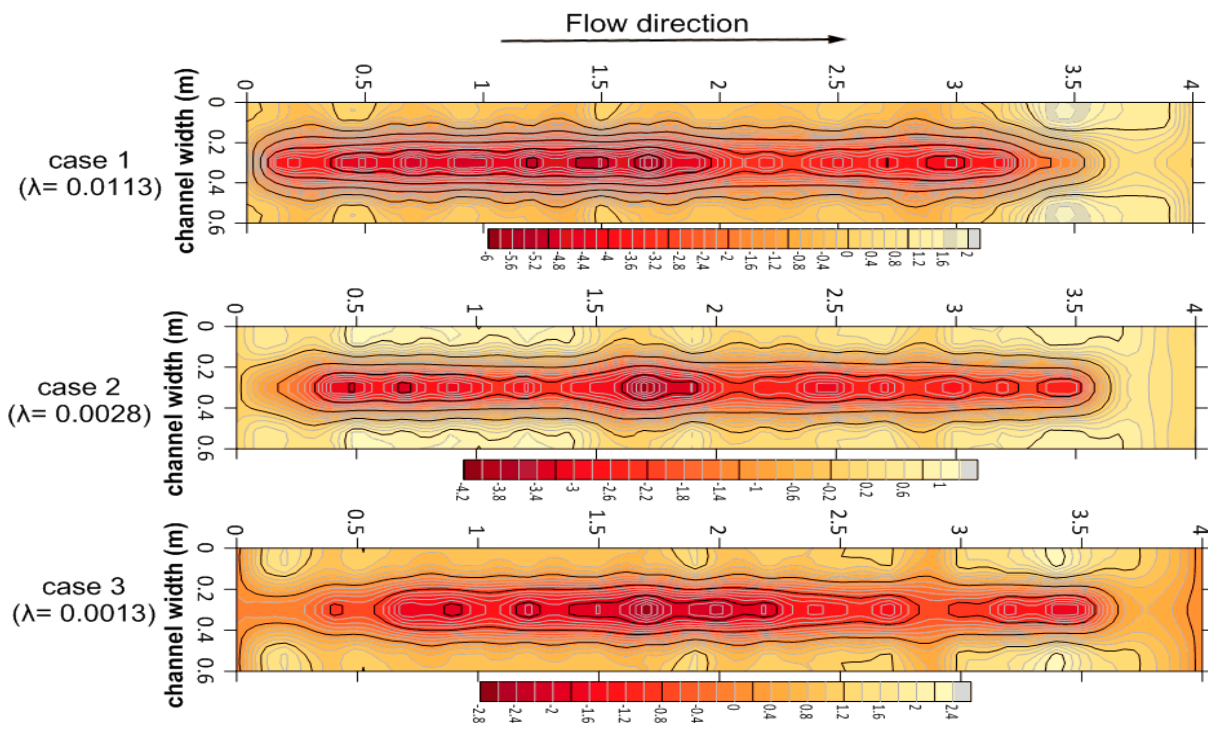


Figure 10. Scour contour map for bilateral weeds at different densities,  $Q = 40$  L/s, and  $F_{r0} = 0.30$ .

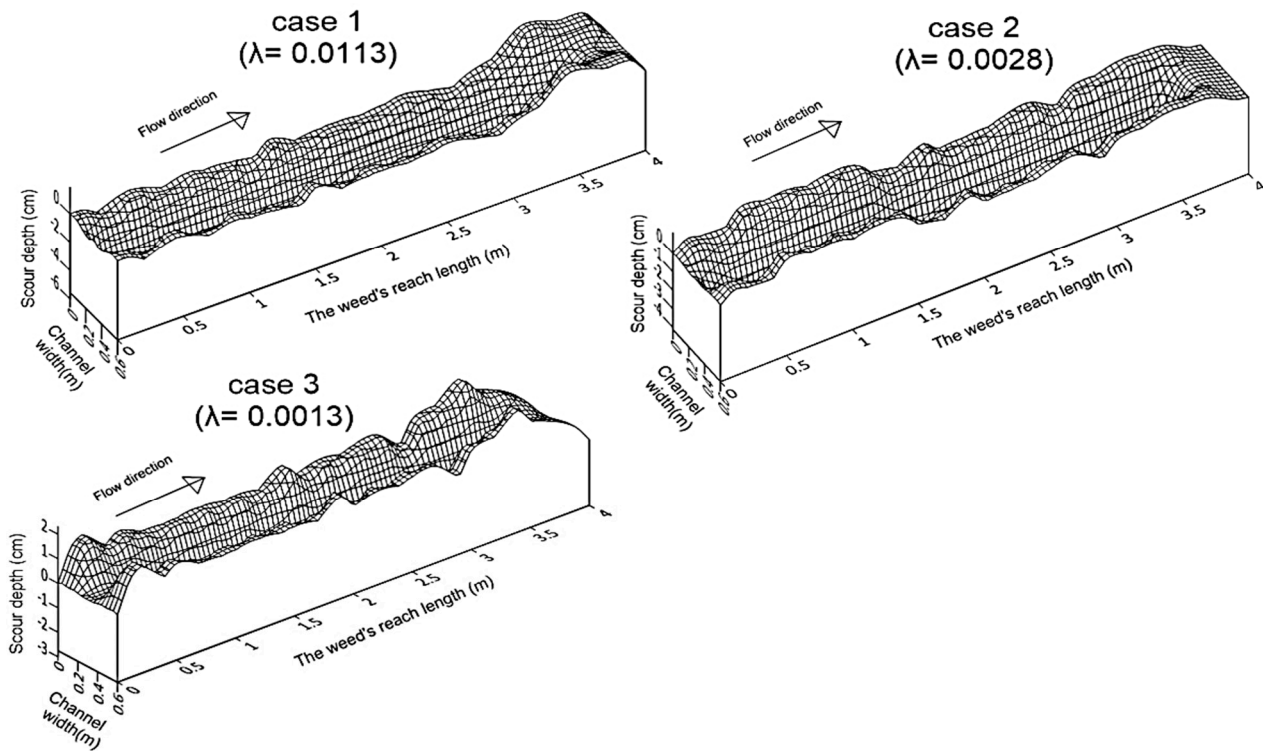


Figure 11. Scour wireframe map for bilateral weeds at different densities,  $Q = 40$  L/s, and  $F_{r0} = 0.30$ .

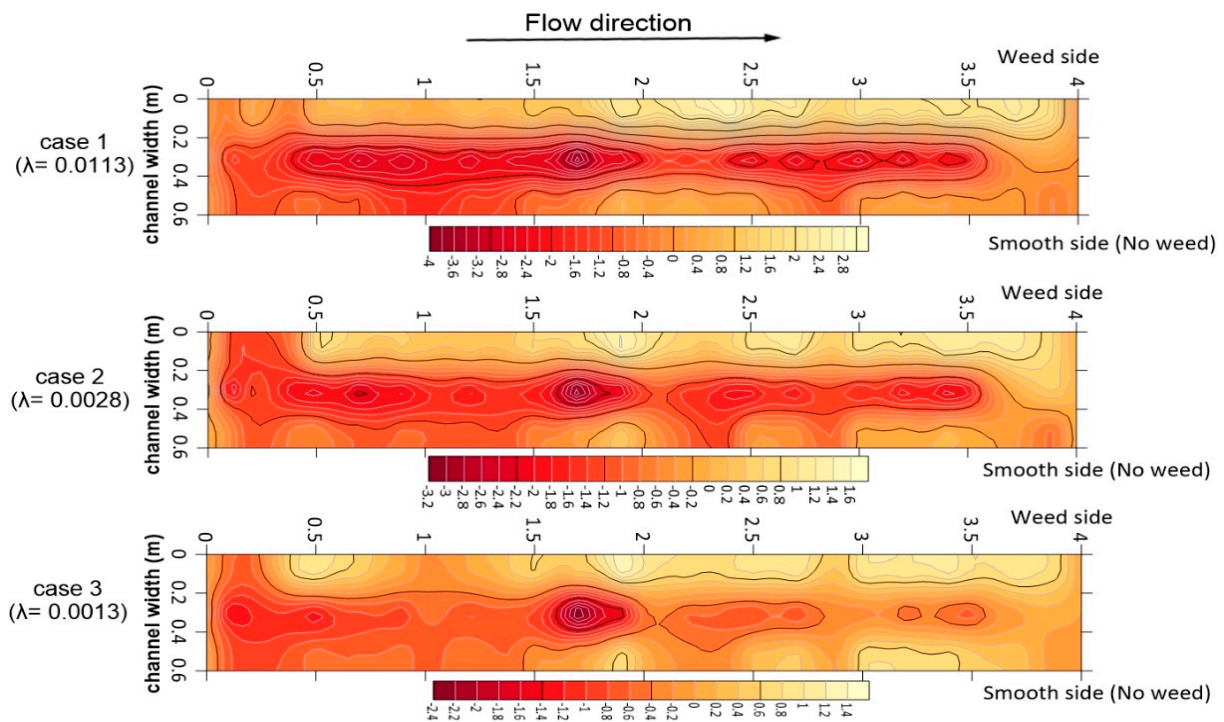


Figure 12. Scour contour map for unilateral weeds at different densities,  $Q = 40 \text{ L/s}$ , and  $Fr_0 = 0.30$ .

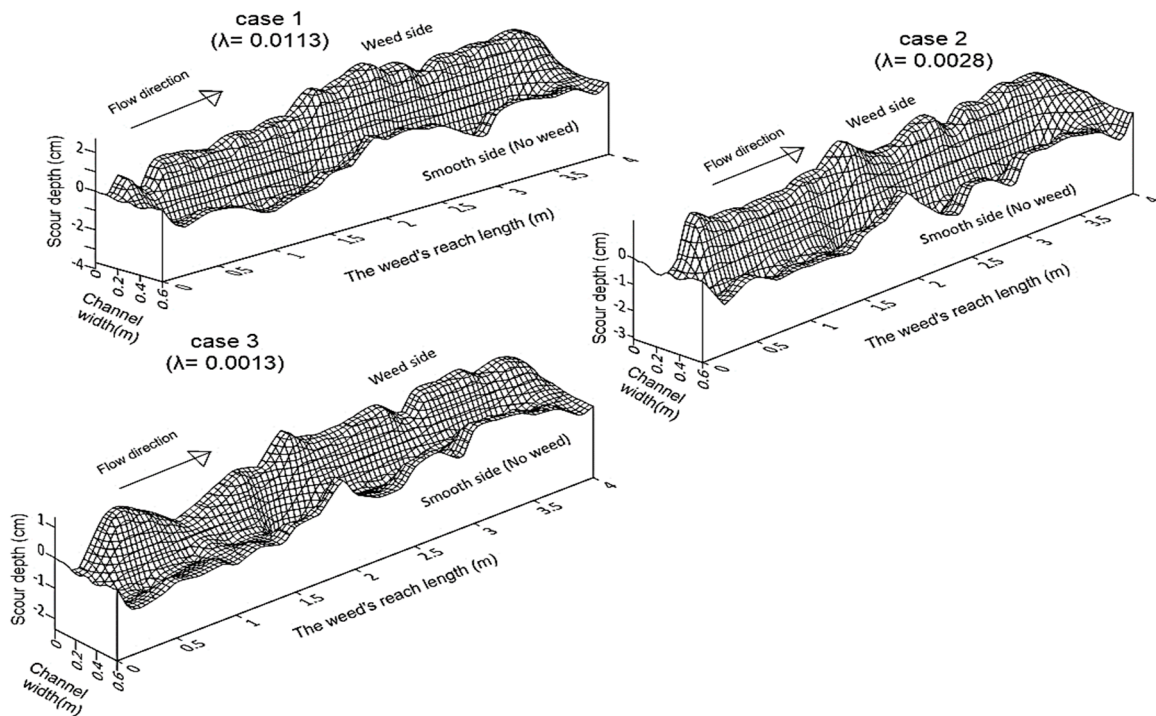
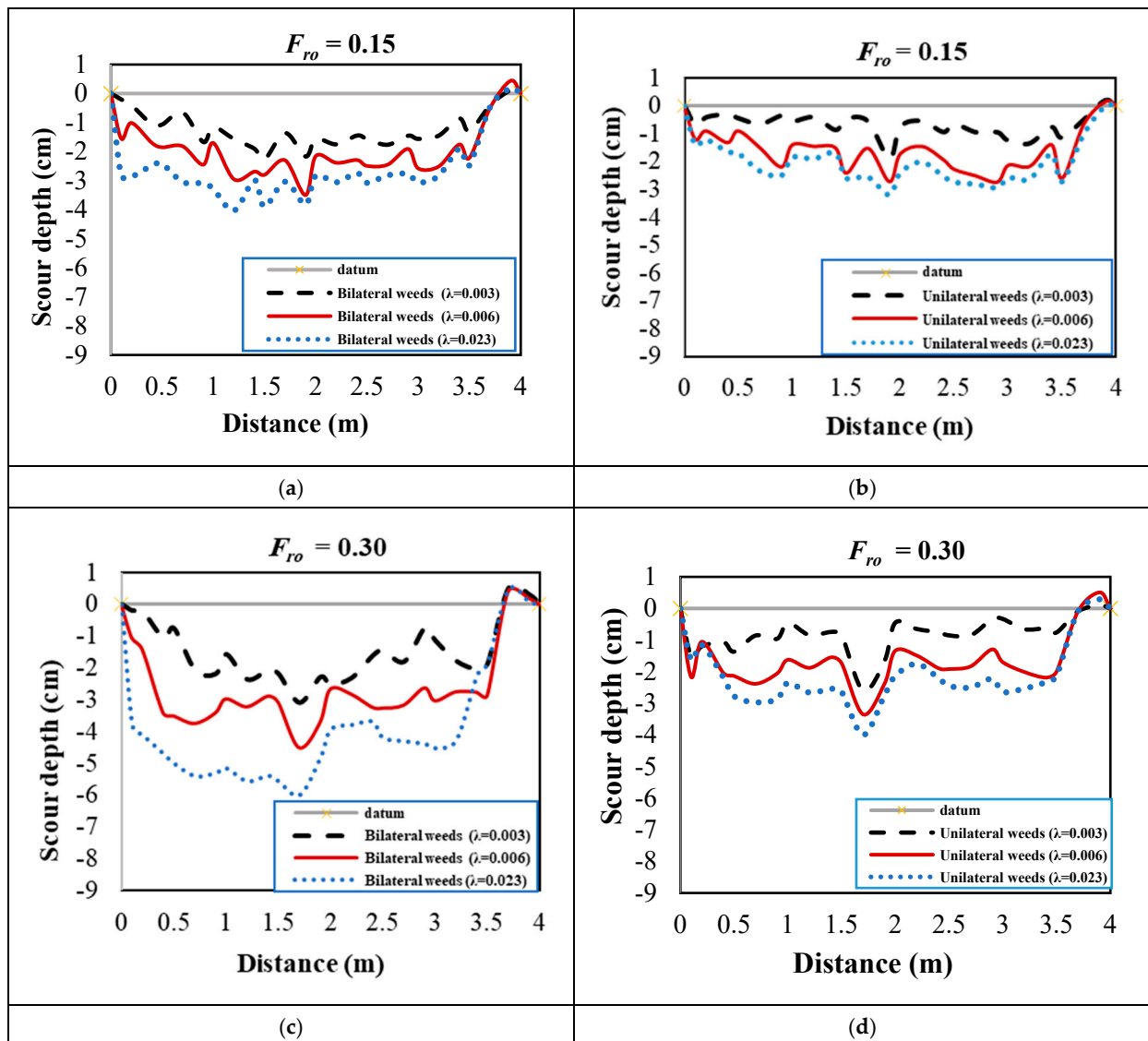


Figure 13. Scour wireframe map for unilateral weeds at different densities,  $Q = 40 \text{ L/s}$ , and  $Fr_0 = 0.30$ .

Although the results proved that bank weeds increase the stability of side slopes, their effect on increasing erosion within the middle of the infested weed reach should not be neglected. Therefore, weed management must be implemented to maintain the channel bed level within permissible levels. Scour profiles along the middle of the weedy reach were plotted for different weeds as a comparison between bilateral and unilateral weeds. Figure 14 shows samples of these plots at different Froude numbers,  $Fr$ .



**Figure 14.** Scour depth along the middle of the vegetation at different densities and  $Q = 40$  L/s for (a,c) bilateral infestation and (b,d) unilateral infestation.

It was indicated that, at the same Froude number, the bilateral distribution gives a higher value of scour depth than the unilateral distribution along the midline of the weedy reach (ranging between 11% and 33%). Also, it was noticed that for all weed distributions, the scour depth increased as  $Fr$  increased. So, the scour depth is a function of the channel geometry and the density of the weeds.

### 3.3. Relative Velocity and Maximum Scour Depth Estimation

Relative velocity and scour depth were estimated as a function of Froude number (in the no-weed case) and weed density as independent variables. The estimation was undertaken using multiple regression analysis, which was performed at a 95% confidence level using Data Fit 9.0 statistical software packages (Oakdale Engineering 2008) [32].  $R^2$  was used as a measure of goodness of fit, where the predicted value indicates how well the model predicts responses to new observations. Before regression, a correlation matrix was produced to show the significant effect of the chosen independent variables on velocity and maximum scour depth (Table 6).

**Table 6.** Correlation matrix for the independent variable and the scour depth.

	$\lambda$	$F_{ro}$	$(V_u/u)_{max}$	$(V_d/u)_{max}$	$(V_{in}/u)_{max}$	$(ds_{max}/y_o)$
$\lambda$	1.00					
$F_{ro}$	0.00	1.00				
$(V_u/u)_{max}$	0.31	0.86	1.00			
$(V_d/u)_{max}$	0.55	0.72	0.93	1.00		
$(V_{in}/u)_{max}$	0.63	0.67	0.90	0.98	1.00	
$(ds_{max}/y_o)$	0.37	0.71	0.73	0.73	0.72	1.00

The correlation matrix shows that both upstream velocity and scour depth are affected more by the channel Froude number than by the density of the weeds.

Under the experimental work limitations, vegetation density ( $\lambda$ ) ranged between 0.013 and 0.0013/m, and the Froude number ( $F_{ro}$ ) ranged between 0.11 and 0.3. Empirical equations were developed to assess and understand the impact of aquatic bank weed density on changes in velocities and scour depth. Table 7 shows the estimated equations and their adjusted coefficient of multiple determination ( $R^2$ ), which is higher than 80%, i.e., there is good fitting quality for the experimental data. Figure 15 shows the fitting curves, where the measured data were plotted against the predicted data. The curves show good fitting for the data, and all data points fall within  $\pm 20\%$ . So, these equations can be used to estimate the change in the velocity and the scour depth.

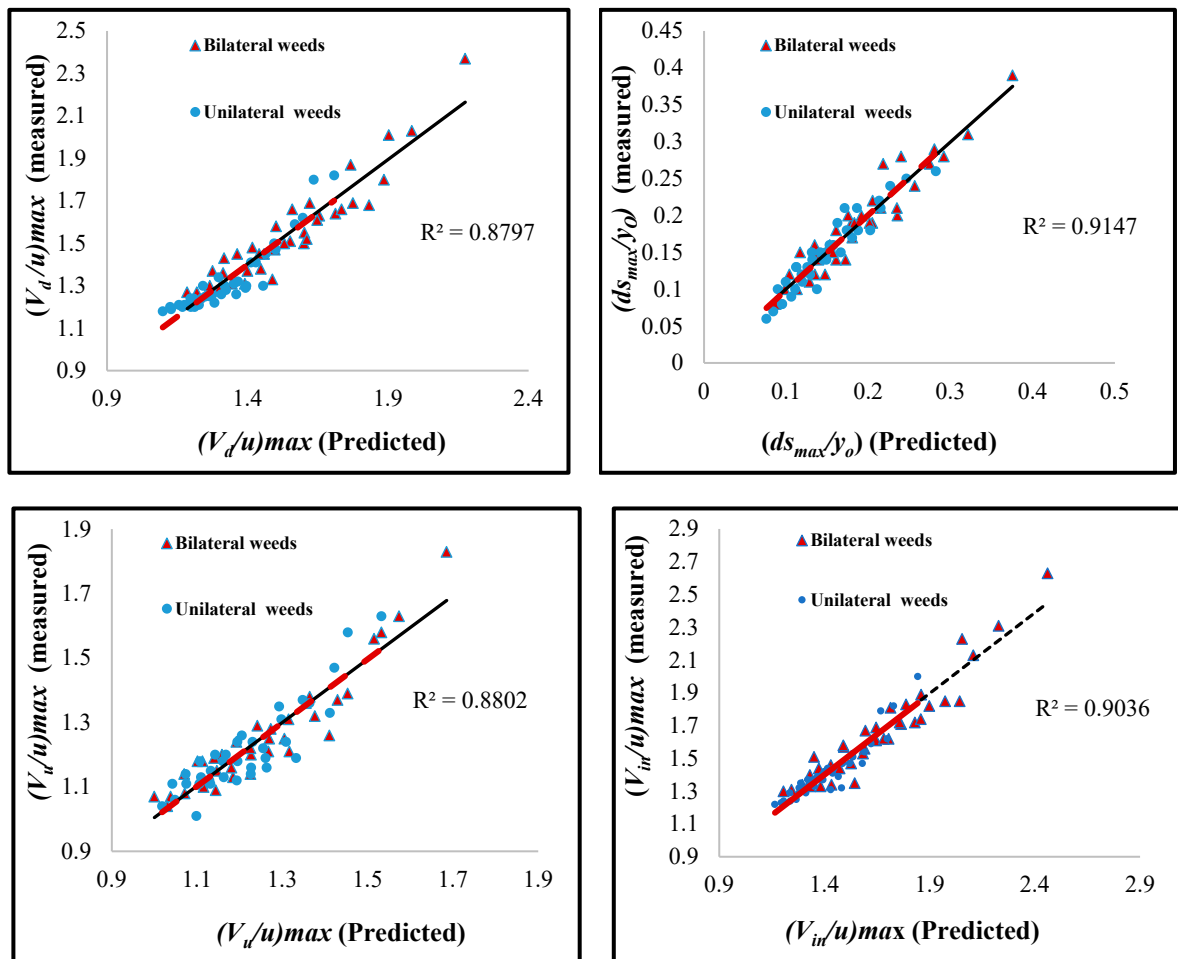


**Figure 15.** Fitting curves for the estimated equations.



**Table 7.** Estimated empirical equations.

Term	Bilateral Weeds	Unilateral Weeds
Upstream relative velocity	$(\frac{V_u}{u})_{max} = 1.10(\lambda)^{0.05} (8.82)^{F_{ro}}$ $R^2 = 0.88$ (3)	$(\frac{V_u}{u})_{max} = 1.10(\lambda)^{0.04} (5.53)^{F_{ro}}$ $R^2 = 0.80$ (4)
Downstream relative velocity	$(\frac{V_d}{u})_{max} = 1.80(\lambda)^{0.1} (8.10)^{F_{ro}}$ $R^2 = 0.88$ (5)	$(\frac{V_d}{u})_{max} = 1.10(\lambda)^{0.03} (7.10)^{F_{ro}}$ $R^2 = 0.85$ (6)
Relative velocity inside the weedy patch	$(\frac{V_{in}}{u})_{max} = 2.24(\lambda)^{0.13} (9.71)^{F_{ro}}$ $R^2 = 0.90$ (7)	$(\frac{V_{in}}{u})_{max} = 1.30(\lambda)^{0.05} (6.57)^{F_{ro}}$ $R^2 = 0.86$ (8)
Relative maximum scour depth	$(\frac{ds_{max}}{y_o}) = 2.70(\lambda)^{0.21} (F_{ro})^{0.96}$ $R^2 = 0.91$ (9)	$(\frac{ds_{max}}{y_o}) = 1.69(\lambda)^{0.20} (F_{ro})^{0.84}$ $R^2 = 0.90$ (10)

### 3.4. Research Application

Detection of changes in velocities, water depths, and bed morphology are important issues in irrigation open-channel management and rehabilitation. So, this research presents a new method for managing channels infested by rigid emerged bank weeds, depending on the numerical formulas that were deduced before. In addition to these formulas (Eraky et al. [15]; Eraky et al. [46]), presented additional numerical formulas that were deduced under the current experimental conditions. These equations estimated the change in water level due to the aquatic bank weeds.

Now, there is a full estimation of the change in flow parameters and bed morphology of open trapezium irrigation channels that are infested by aquatic weeds along their sides. This estimation will contribute to irrigation channel management and rehabilitation, offering a chance to carry them out with the minimum expenditure of time and money.

## 4. Conclusions

The authors studied the effect of rigid aquatic bank weeds on flow velocity and bed morphology under sub-critical flow conditions at different discharge rates and weed densities in a trapezoidal open channel. The conclusions drawn are as follows:

The measured velocities increased with increased weed density and correlated directly with the Froude number ( $F_{ro}$ ). The maximum velocity occurred within the weedy reach and was close to that measured just downstream of the weedy reach.

The maximum velocity in the center of the infested reach occurred in the lower half of the water column ( $y/h_o \leq 0.5$ ).

It was found that for all weed distributions, increasing  $Fr$  and vegetation density increased the scour depth.

For bilateral weeds, the averages of the maximum velocity-increasing ratios were 5%, 36%, and 32% for upstream, middle, and downstream velocities, respectively. The bilateral distribution gave a higher value of scour depth than the unilateral distribution along the midline of the weedy reach (ranging between 11% and 33%).

For unilateral weeds, the averages of the maximum velocity-increasing ratios were 2%, 16%, and 11% for upstream, middle, and downstream velocities, respectively. Generally, the effect of the unilateral weeds on flow velocities and channel morphology was less than that of the distribution of the bilateral weeds.

Due to the pushing flow, the smooth bank was exposed to erosion. The maximum observed depth of scour holes along the smooth bank was about 30% to 60% of the maximum scour depth that occurred at the middle line.

Aquatic bank weeds pushed the flow toward the canal center, leading to an increased velocity in the center that was greater than that in the region near the bank. This led to increased scour in the center rather than in the near-bank region.

Although the results conformed to the knowledge that bank weeds increase the stability of side slopes, their effect on increasing bed scour within the middle of the weedy

reach should not be neglected. Therefore, weeds must be managed to maintain the channel bed level within permissible levels.

Under the experimental work limitations, in which vegetation density ( $\lambda$ ) ranged between 0.013 and 0.0013/m and Froude number ( $F_{ro}$ ) ranged from 0.11 to 0.30, eight empirical equations were developed to assess and understand the impact of aquatic bank weed density on changes in velocities and scour. These equations can contribute to irrigation channel management and rehabilitation, offering a chance to carry them out with the minimum expenditure of time and money.

According to [9], this research presented the effect of bank weeds on the flow parameters for narrow channels in which the ratio between channel width and height is less than 5. Therefore, it is recommended that further studies investigate the effect of bank weeds on flow parameters in wide channels. Also, it is advisable to study the effects of sparse distribution and denser vegetation conditions.

**Author Contributions:** Conceptualization, M.S.A. and O.M.E.; methodology, M.S.A., O.M.E. and E.F.M.E.; experiments, O.M.E. and M.S.A.; formal analysis, O.M.E., M.A.R.E. and E.F.M.E.; investigation, I.G.S. and M.A.R.E.; data curation, O.M.E., M.S.A. and E.F.M.E.; writing—original draft preparation, O.M.E. and I.G.S.; writing—review and editing, E.F.M.E. and I.G.S. All authors have read and agreed to the published version of the manuscript.

**Funding:** This research received no external funding.

**Data Availability Statement:** The data are available from the first author upon reasonable request.

**Acknowledgments:** The experimental work was carried out in the hydraulic lab of the channel maintenance research institute, NWRC. The authors wish to express their gratitude to the institute director and the technical staff of the hydraulic laboratory for their sincere efforts throughout this work.

**Conflicts of Interest:** The authors have declared that no competing interest exist.

## References

- Galema, A.A. Vegetation Resistance Evaluation of Vegetation Resistance Descriptors for Flood Management. Master's Thesis, University of Twente, Enschede, The Netherlands, 2009.
- El Samman, T.A.; El Ella, S.M.A. Aquatic weeds monitoring and associated problems in Egyptian Channels. In Proceedings of the Thirteenth International Water Technology Conference, Hurghada, Egypt, 12–15 March 2009.
- Kemp, J.L.; Harper, D.M.; Crosa, G.A. The habitat-scale eco-hydraulics of rivers. *J. Ecol. Eng. JEE* **2000**, *16*, 17–29. [[CrossRef](#)]
- Tang, H.; Lu, S.; Zhou, Y.; Xu, X.; Xiao, Y. Water environment improvements in Zhenjiang City, China. *ICE-Munic. Eng.* **2008**, *161*, 11–16. [[CrossRef](#)]
- Nepf, H.M. Hydrodynamics of Vegetated Channels. *J. Hydraul. Resour.* **2012**, *50*, 262–279. [[CrossRef](#)]
- Kim, H.S.; Nabi, M.; Kimura, I. Computational modeling of flow and morphodynamics through rigid-emergent vegetation. *Adv. Water Resour.* **2015**, *84*, 64–86. [[CrossRef](#)]
- Xu, Z.X.; Ye, C.; Zhang, Y. 2D Numerical Analysis of the Influence of Near-Bank Vegetation Patches on the Bed Morphological Adjustment. In *Environmental Fluid Mechanics*; Springer: Berlin/Heidelberg, Germany, 2020. [[CrossRef](#)]
- Hopkinson, L.C.; Wynn-Thompson, T.M. Comparison of direct and indirect boundary shear stress measurements along vegetated streambanks. *River Res. Appl.* **2016**, *32*, 1755–1764. [[CrossRef](#)]
- Afzalimehr, H.; Dey, S. Influence of bank vegetation and gravel bed on velocity and Reynolds stress distributions. *Int. J. Sediment Res.* **2009**, *24*, 236–246. [[CrossRef](#)]
- Hirschowitz, P.M.; James, C.S. Conveyance estimation in channels with emergent bank vegetation. *Water SA* **2009**, *35*, 607–614. [[CrossRef](#)]
- Afzalimehr, H.; Fazel, N.E.; Singh, V.P. Effect of Vegetation on Banks on Distributions of Velocity and Reynolds Stress under Accelerating Flow. *J. Hydrol. Eng. ASCE* **2010**, *15*, 708–713. [[CrossRef](#)]
- Mohammadzade, N.; Afzalimehr, H.; Singh, V.P. Experimental Investigation of Influence of Vegetation on Flow Turbulence. *Int. J. Hydraul. Eng.* **2016**, *4*, 54–69. [[CrossRef](#)]
- Liu, D.; Valyrakis, M.; Williams, R. Flow Hydrodynamics across Open Channel Flows with Riparian Zones: Implications for Riverbank Stability. *Water* **2017**, *9*, 720. [[CrossRef](#)]
- Valyrakis, M.; Liu, D.; Turker, U. The role of increasing riverbank vegetation density on flow dynamics across an asymmetrical channel. *Environ. Fluid Mech.* **2021**, *21*, 643–666. [[CrossRef](#)]
- Eraky, O.M.; Eltoukhy, M.A.; Abdelmoaty, M.S. Effect of rigid, bank vegetation on velocity distribution and water surface profile in open channel. *Water Pract. Technol.* **2022**, *17*, 1445–1457. [[CrossRef](#)]

16. James, C.S.; Birkhead, A.L.; Jordanova, A.A.; O'Sullivan, J.J. Flow resistance of emergent vegetation. *J. Hydraul. Res.* **2004**, *42*, 390–398. [[CrossRef](#)]
17. Huai, W.X.; Chen, Z.B.; Jie, H.A.N.; Zhang, L.X.; Zeng, Y.H. Mathematical model for the flow with submerged and emerged rigid vegetation. *J. Hydrodyn. Ser. B* **2009**, *21*, 722–729. [[CrossRef](#)]
18. Liu, C.; Shan, Y. Impact of an emergent model vegetation patch on flow adjustment and velocity. *Proc. Inst. Civ. Eng. Water Manag.* **2022**, *175*, 55–66. [[CrossRef](#)]
19. Van de Lageweg, W.I.; van Dijk, W.M.; Hoendervoogt, R. Effects of riparian vegetation on experimental channel dynamics. In *International Conference on Fluvial Hydraulics: River Flow*; Bundesanstalt für Wasserbau Braunschweig: Karlsruhe, Germany, 2010.
20. Yang, S.; Bai, Y.; Xu, H. Experimental analysis of river evolution with riparian vegetation. *Water* **2018**, *10*, 1500. [[CrossRef](#)]
21. Abdelhaleem, F.S.; Mohamed, I.M.; Shaaban, I.G.; Ardakanian, A.; Fahmy, W.; Ibrahim, A. Pressure-Flow Scour under a Bridge Deck in Clear Water Conditions. *Water* **2023**, *15*, 404. [[CrossRef](#)]
22. Li, J.F.; Tfwala, S.S.; Chen, S.C. Effects of vegetation density and arrangement on sediment budget in a sediment-laden flow. *Water* **2018**, *10*, 1412. [[CrossRef](#)]
23. Vargas-Luna, A.; Crosato, A.; Calvani, G. Representing plants as rigid cylinders in experiments and models. *Adv. Water Resour.* **2016**, *93*, 205–222. [[CrossRef](#)]
24. Vargas-Luna, A.; Duró, G.; Crosato, A. Morphological Adaptation of River Channels to Vegetation Establishment: A Laboratory Study. *J. Geophys. Res. Earth Surf.* **2019**, *124*, 1981–1995. [[CrossRef](#)]
25. Azarisamani, A.; Keshavarzi, A.; Hamidifar, H.; Javan, M. Effect of rigid vegetation on velocity distribution and bed topography in a meandering river with a sloping bank. *Arab. J. Sci. Eng.* **2020**, *45*, 8633–8653. [[CrossRef](#)]
26. Schoneboom, T.; Aberle, J.; Dittrich, A. Spatial variability, mean drag forces, and drag coefficients in an array of rigid cylinders. In *Experimental Methods in Hydraulic Research*; Rowinski, P., Ed.; Springer: Berlin/Heidelberg, Germany, 2011; Volume 1, pp. 255–265.
27. Jumain, M.; Ibrahim, Z.; Ismail, Z. Hydraulic and morphological patterns in a riparian vegetated sandy compound straight channel. *IOP Conf. Ser. Earth Environ. Sci.* **2021**, *646*, 012036. [[CrossRef](#)]
28. Stone, B.M.; Shen, H.T. Hydraulic resistance of flow in channels with cylindrical roughness. *J. Hydraul. Eng.* **2002**, *128*, 500–506. [[CrossRef](#)]
29. Meftah, M.B.; De Serio, F.; Malcangio, D.; Perrillo, A.F.; Mossa, M. Experimental study of flexible and rigid vegetation in an open channel. In Proceedings of the River Flow Conference on Fluvial Hydraulics, River Flow, Lisbon, Portugal, 6–8 September 2006; Volume 1, pp. 603–611.
30. Kothyari, U.C.; Hayashi, K.; Hashimoto, H. Drag coefficient of unsubmerged rigid vegetation stems in open-channel flows. *J. Hydraul. Res.* **2009**, *47*, 691–699. [[CrossRef](#)]
31. Cheng, N.S.; Nguyen, H.T. Hydraulic radius for evaluating resistance induced by simulated emergent vegetation in open-channel flows. *J. Hydraul. Eng.* **2011**, *137*, 995–1004. [[CrossRef](#)]
32. Panigrahi, K. Experimental Study of Flow-Through Rigid Vegetation in Open Channel. Master's Thesis, National Institute of Technology, Rourkela, Odisha, India, 2015.
33. Ahmed, M.; Hady, A. Evaluation of emergent vegetation resistance and comparative study between last descriptors. *Control Sci. Eng.* **2017**, *1*, 1–7.
34. Chakraborty, P.; Sarkar, A. Study of flow characteristics within randomly distributed submerged rigid vegetation. *J. Hydrodyn.* **2018**, *31*, 358–367. [[CrossRef](#)]
35. Tong, X.; Liu, X.; Yang, T.; Hua, Z.; Wang, Z.; Liu, J.; Li, R. Hydraulic features of flow through local non-submerged rigid vegetation in the Y-shaped confluence channel. *Water* **2019**, *11*, 146. [[CrossRef](#)]
36. D'Ippolito, A.; Calomino, F.; Penna, N.; Dey, S.; Gaudio, R. Simulation of Accelerated Subcritical Flow Profiles in an Open Channel with Emergent Rigid Vegetation. *Appl. Sci.* **2022**, *12*, 6960. [[CrossRef](#)]
37. Lee, J.; Jeong, Y.M.; Kim, J.S.; Hur, D.S. Analysis of hydraulic characteristics according to the cross-section changes in submerged rigid vegetation. *J. Ocean Eng. Technol.* **2022**, *36*, 326–339. [[CrossRef](#)]
38. Wang, Q.; Zhang, Y.; Wang, P.; Feng, T.; Bai, Y. Longitudinal velocity profile of flows in open channel with double-layered rigid vegetation. *Front. Environ. Sci.* **2023**, *10*, 1094572. [[CrossRef](#)]
39. Huang, T.; He, M.; Hong, K.; Lin, Y.; Jiao, P. Effect of Rigid Vegetation Arrangement on the Mixed Layer of Curved Channel Flow. *J. Mar. Sci. Eng.* **2023**, *11*, 213. [[CrossRef](#)]
40. Li, J.; Claude, N.; Tassi, P.; Cordier, F.; Vargas-Luna, A.; Crosato, A.; Rodrigues, S. Effects of vegetation patch patterns on channel morphology: A numerical study. *J. Geophys. Res. Earth Surf.* **2022**, *127*, e2021JF006529. [[CrossRef](#)]
41. Lin, Y.-T.; Ye, Y.-Q.; Han, D.-R.; Chiu, Y.-J. Propagation and Separation of Down slope Gravity Currents over Rigid and Emergent Vegetation Patches in Linearly Stratified Environments. *J. Mar. Sci. Eng.* **2022**, *10*, 308. [[CrossRef](#)]
42. Mofrad, M.R.T.; Afzalimehr, H.; Parvizi, P.; Ahmad, S. Comparison of Velocity and Reynolds Stress Distributions in a Straight Rectangular Channel with Submerged and Emergent Vegetation. *Water* **2023**, *15*, 2435. [[CrossRef](#)]
43. Dey, S.; Raikar, R.V.; Roy, A. Scour at submerged cylindrical obstacles under steady flow. *J. Hydraul. Eng.* **2008**, *134*, 105–109. [[CrossRef](#)]
44. Devi, T.B.; Kumar, B. Experimentation on submerged flow over flexible vegetation patches with downward seepage. *Ecol. Eng.* **2016**, *91*, 158–168. [[CrossRef](#)]

45. Amir, M.U.; Hashmi, H.N.; Baloch, M. Experimental investigation of channel bank vegetation on scouring characteristics around a wing wall abutment. *Tech. J. Univ. Eng. Technol. UET* **2018**, *23*, 15–21.
46. Eraky, O.M.; Eltoukhy, M.A.; Abdelmoaty, M.S. Heading Up and Head Losses Estimation Due to Rigid Bank Vegetation. *Eng. Res. J. ERJ* **2023**, *52*, 64–72. [[CrossRef](#)]

**Disclaimer/Publisher's Note:** The statements, opinions and data contained in all publications are solely those of the individual author(s) and contributor(s) and not of MDPI and/or the editor(s). MDPI and/or the editor(s) disclaim responsibility for any injury to people or property resulting from any ideas, methods, instructions or products referred to in the content.